

CORRECTION OF INFLUENCES ON THERMOGRAPHIC MEASUREMENTS FOR NON-CONTACT TEMPERATURE MEASUREMENT USING INFRARED THERMOGRAPHY

^{1,2,*}Faouaz JEFFALI, ¹Bachir EL KIHHEL, ²Abdelkarim NOUGAOUI, ^{2,3}Abdelhamid KERKOUR-EL MIAD, ⁴Fabienne DELAUNOIS

¹Laboratoire de Génie Industriel et Production Mécanique, École Nationale des Sciences Appliquées, Université Mohamed Premier, B.P. 524, 6000, Oujda-Maroc

²Laboratoire de Dynamique et d'Optique des Matériaux, Faculté des Sciences, Université Mohamed Premier, B.P. 524, 6000, Oujda, Maroc

³École Nationale des Sciences Appliquées Al Hoceima, BP 03 Ajdir-Al Hoceima, Université Mohamed Premier, B.P. 524, 6000, Oujda-Maroc

⁴Laboratoire de Métallurgie, Polytechnique, Mons-Belgique

E-mail: *f.jeffali@ump.ac.ma

ABSTRACT

The diagnostics failures of monitoring the condition of rotation machinery in the industry are considered very significant to ensure the efficiency and safety of production. However, many serious malfunctioning to the machine could easily occur because of these failures, thus, a huge shortage in production. In this domain, In fact, the most important installation faults lead to an increase of temperature in specific areas. Infrared Thermography is a technique that has been used regularly as a predictive device for the maintenance of electrical installations. It is used around the field in order to evaluate the condition of electrical systems and equipment. This article presents information about issues that demand a specific focus during thermal tests of induction motor. Which are presented as errors that could be made at the testing phase, and especially the descriptions of the influences of parameters, on Thermographic measurements that are obtained by a conversion of raw data to digital data by the use of Flir Tools Software.

Keywords: *Thermography Camera, Moteur Asynchrone, Powder Brake, Effect Of Factors, Temperature Measurement, Thermal Image.*

1. INTRODUCTION

Nowadays many existing industrial induction motors fault diagnosis techniques depend on the analysis of quantities like currents or vibrations [1]. Vibration-based condition monitoring is also spread in the industry, due to its ability to diagnose many failures with a mechanical origin [2]-[3]. Yet, it often requires the installation of sensors and transducers, which is not always a possible option without perturbing the operation of the machine. In any case, neither current nor vibration analysis enables the diagnosis of all possible failures occurring in induction motors. There are some faults (stator short-circuits) which are difficult to be diagnosed with any of the previous quantities, while other (bearing failures, very common in induction motors) could be detected by monitoring

vibration signals which, as commented above, are not always available [4]-[5]-[6]-[7].

In this context, infrared thermography plays the important role of identifying and analyzing thermal anomalies for condition monitoring of machines. Infrared thermography works as follows, it measures the distribution of radiant thermal energy (heat) emitted from a target surface and converts the latter to a surface temperature map or thermogram. In thermography, a thermal imaging infrared camera is used to scan, monitor and detect the infrared emissions from the surface and generate thermal patterns or uneven heat distribution of the scanned area. These scanned images are very convenient in detecting incipient fault and deterioration in the equipment caused by overheating due to defect [8]-[9]-[10].

This article provides information about issues that require specific focus during thermal tests of induction motor. Which are presented as errors that could be possibly made at the testing phase, and especially the descriptions of the influences of parameters, on thermographic measurements that are obtained by a conversion of raw data to digital data by the use of Flir Tools Software? All the measurements performed at the technological platform PFT2M, Industrial Engineering Laboratory and Mechanical Production of the ENSA-Department of Industrial in Oujda.

2. THEORETICAL BACKGROUND

The infrared thermographic camera can capture a thermal pattern's image as well as be used in different temperature ranges depending on the emissivity of the surface. A thermogram then is the thermographic digital image which is captured by the camera. Every pixel of a thermogram has an exact temperature value, and the contrast of the image is derived from the differences in temperature of the object surface [11]. It can occur in levels of gray. The color assignment for each degree of temperature is based on a palette of colors with which it is allowed to view the temperature of the object. In addition Segmentation is capable of analyzing a specific hot spot through a two-dimensional signal that is provided by the infrared thermographic analysis.

The relationship in which Infrared thermography exploits the correlation between the temperature of a surface and also the IR energy which is emitted by the surface is here described by Stefan's Law [12]:

$$W_{BB}(\lambda, T) = \sigma T^4 \tag{1}$$

Yet, it radiates a portion of it, characterized by its emissivity

$$W_{GB}(\lambda, T) = \epsilon \sigma T^4 \tag{2}$$

The precision of the object temperature which is estimated by the thermographic camera is usually tightly linked to the accuracy of evaluation of input parameters. The emissivity value of the object needs to be determined accurately since it is the most important parameter [13]-[16].

3. SOFTWARE OF THERMAL DATA

FLIR TOOLS is the image processing tool that helps us extract the temperature values that are registered on a Flir image file which allows us to analyze the raw data recorded by infrared camera and convert them into digital data used in the validation process. Conversion errors are at the order errors due to a multiplication of 64 bits which remain negligible. The following figure.1 shows us a preview of FLIR Tools Software.

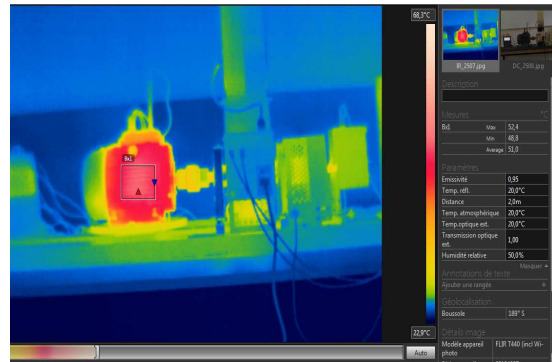


FIGURE.1. Software to analyze data

4. EFFECT OF FACTORS

Temperature of the atmosphere: can modify the actual temperature of an object. By definition this is the temperature of the air between the camera and the object of interest [15].

Reflected temperature: can change the actual temperature of object. In a case the background has more emissivity than the target object. Then infrared camera will see the background hotter than the target. In another case where the target object has more emissivity, then the latter shall be hotter than the background [14]-[15].

Relative humidity: is the amount of water in the air at any particular temperature relative to the saturation level. It also has minimal effect on object temperature measurement and increases with the object temperature [14]-[15].

5. EXPERIMENT AND MEASUREMENTS

5.1. Experimental setup

Figure.2. was constructed in the technological platform PFT2M, Industrial Engineering Laboratory and Mechanical Production of the ENSA-Department of Industrial in Oujda. Figure.3 demonstrates a view of the experimental set-up with all the measurement devices. It is composed of a three-phase motor group with an encoder fixed on a baseplate. The motor controller

consists of a frequency converter destined to adjust progressively the running speed. In addition of having a running speed indicator and an indicator of the power absorbed by the motor.

Powder brake principle: The DC current injected into the brake coil creates a field which causes the magnetic powder placed in the air gap to agglomerate. The braking torque is proportional to the field current alone; in particular it is independent of the speed of rotation. Waste heat is eliminated by forced ventilation. A circuit breaker cuts the field current in the event of the brake overheating. This brake is always mounted in balance so that it can be equipped with a static sensor with a strain gauge. Listed in Table.3 are the main specifications of the Powder brake are.

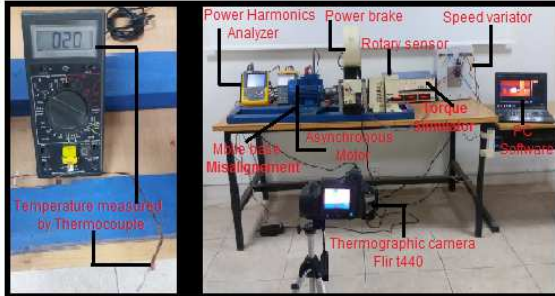


Figure.2 Experimental mounting.

5.2. Experimental procedure

In this experiment, Table.1 lists the main specifications of the thermal camera. The thermographic system communicates with PC which is later processed in the suitable analyzing software. In this work presented the temperature of the windings in a 3-phase motor realized under different load conditions (Figure.1). The technical specifications of the motor are shown in Table.2.

Table.1. Technical characteristics of the Thermographic camera used in this paper

| Description | Value |
|-----------------------------|---|
| Model Name | Flir t440 |
| Temperature measuring range | -20 °C to 1200 °C |
| Emissivity | Correction variable from 0.01 to 1.0 or selected from list of materials |
| Image frequency | 60Hz |
| Spectral range | 7.5 to 13um |
| Detector | Focal plane array uncooled microbolometer,320 x 240 pixels |
| Thermal sensitivity | <0.045°C at 30°C |

Table.2. Parameters of Induction motor

| Parameter | Value |
|--------------------|-----------------------------|
| Rated Power | 0.55 kW |
| Rated power factor | 0.73 |
| Rated Speed | 1360 RPM |
| Power Supply | Three phase 230/400 V 50 Hz |
| Maximal torque | 3.5Nm |

Table.3. Technical characteristics of brake settings

| Parameter | Value |
|----------------------------------|------------|
| Max torque | 65Nm |
| Weight | 21kg |
| Voltage/Current max for blocking | 10V / 0.5A |

The thermal images are shown in Figure.3 which carrying only visual inspection of machine condition. Figure.4. shows the data structure from Tools software to analyze data in Celsius scale which has been processed for diagnosis of the frame motor after 60 minutes.

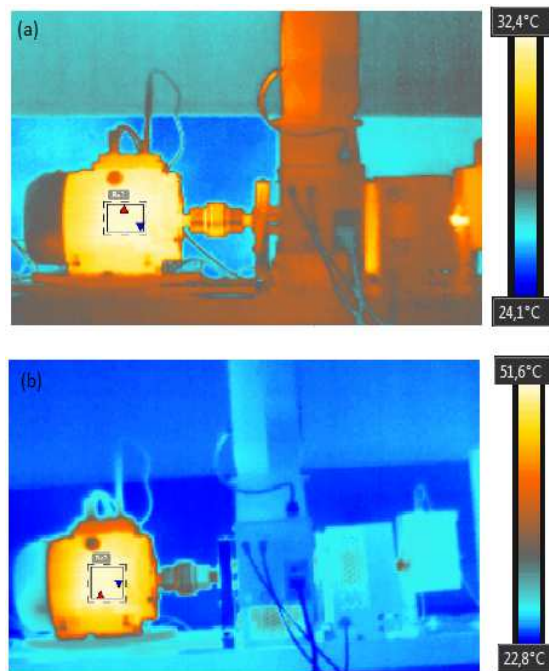


Figure.3. (a) The thermal image of the frame motor after 60 minutes of operation for without load, (b) The thermal image of the frame motor after 60 minutes of operation for full load with the braking torque [2.5Nm].

Table.7. The Atmospheric Temperature And Relative Humidity Influence On Surface Temperature Measurements For Full Load [2.5Nm] After 10 Minutes

| Relative humidity [%] | Maximum measure temperature $T_{max} [^{\circ}C]$ |
|---|---|
| 20% | 43.16 |
| 30% | 43.42 |
| 40% | 43.96 |
| 50% | 44.24 |
| 75% | 44.81 |
| 90% | 45.10 |
| 100% | 45.40 |
| Atmospheric temperature $T_{atm} [^{\circ}C]$ | Maximum measure temperature $T_{max} [^{\circ}C]$ |
| +05 | 43.63 |
| +10 | 42.99 |
| +15 | 42.32 |
| +20 | 41.60 |
| -20 | 46.30 |
| -15 | 45.83 |
| -10 | 45.33 |
| -05 | 44.80 |

Table.8. The Atmospheric Temperature And Relative Humidity Influence On Surface Temperature Measurements For Full Load [2.5Nm] After 60 Minutes

| Relative humidity [%] | Maximum measure temperature $T_{max} [^{\circ}C]$ |
|---|---|
| 20% | 51.67 |
| 30% | 52.10 |
| 40% | 52.96 |
| 50% | 53.42 |
| 75% | 54.95 |
| 90% | 55.28 |
| 100% | 55.77 |
| Atmospheric temperature $T_{atm} [^{\circ}C]$ | Maximum measure temperature $T_{max} [^{\circ}C]$ |
| +05 | 52.90 |
| +10 | 52.37 |
| +15 | 51.80 |
| +20 | 51.20 |
| -20 | 55.15 |
| -15 | 54.76 |
| -10 | 54.34 |
| -05 | 53.89 |

6.1. Surface temperature for different emissivity and temperature reflection

The Thermogram of measurement in figure.5 confirms that the emissivity is not a great influence on the measurement if the temperature of reflection is close to ambient temperature. The temperature of reflection will be more influential than the emissivity (for high emissivity), depending on the environment of the measure. This is a statement that is clearly shown in table.9. And in order to get the correct values parameters for this whole operation check table.10.

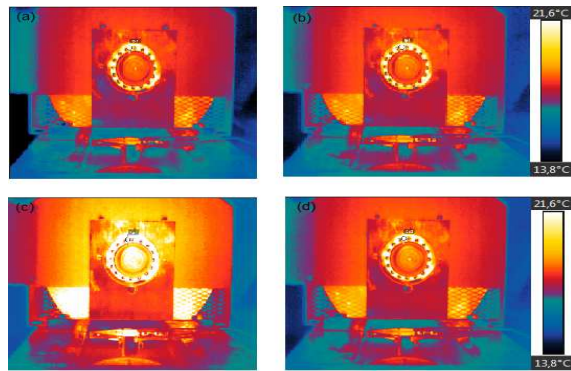


Figure.5. Thermogram Of Measurement With:

- (a) : $\epsilon = 0,90$; $T_{refl} = 20^{\circ}C$; $T_{amb} = 20^{\circ}C$
- (b) : $\epsilon = 0,98$; $T_{refl} = 20^{\circ}C$; $T_{amb} = 20^{\circ}C$
- (c) : $\epsilon = 0,90$; $T_{refl} = -15^{\circ}C$; $T_{amb} = 20^{\circ}C$
- (d) : $\epsilon = 0,98$; $T_{refl} = -15^{\circ}C$; $T_{amb} = 20^{\circ}C$

Table.9. Surface Temperature Variation For Different Emissivity And Reflection Temperature

| Determining the surface temperature area of SP01 | | | |
|--|------------------|-------------------|-------------------|
| Reflected temperature $T_{refl} [^{\circ}C]$ | $\epsilon = 0.9$ | $\epsilon = 0.95$ | $\epsilon = 0.98$ |
| -45 | 27 | 24,4 | 22,9 |
| -15 | 25,3 | 23,6 | 22,6 |
| 0 | 24,1 | 23 | 22,4 |
| 20 | 22,2 | 22,1 | 22 |

Table.10. Correct Values Parameters (SP01)

| Correct parameters | Values | T_{max} [$^{\circ}C$] | T_{min} [$^{\circ}C$] |
|--------------------------------|-----------------|---------------------------|---------------------------|
| Emissivity | 0.95 | 52.40 | 50.30 |
| Reflected apparent temperature | +20 $^{\circ}C$ | | |
| Object distance | 1m | | |
| Atmospheric temperature | +20 $^{\circ}C$ | | |
| Relative humidity | 50% | | |
| Ambient temperature laboratory | 20 $^{\circ}C$ | | |



Figure.6. Thermal Image (Thermogram) With Correct Parameters, 60minutes Of Continues Operation With The Braking Torque [2.5Nm] Set In Camera FLIR T440. (See Table.9)

The engine was tested under different conditions. The first test is the measurement of the engine temperature at no load. In Figure.7 we see how the maximum temperature measured increases every minute for a continuous operation of a total 60 minutes. From the measurements, it is clear that the temperature increases rapidly during the first 30 minutes then with a slower pace for the next few minutes.

In order to find the effects of environmental factors on the infrared temperature measurement, Figure-8 shows how the maximum values are measured for changes in the values of the actual atmospheric temperature. Similarly, we find that incorrect values on an atmospheric temperature have little influence on the measurement results. Figure-9 shows how defective relative humidity affects the thermographic results. Again, the correct moisture content has little influence on the thermographic measurements. Details of how the atmospheric temperature and the relative humidity harm alter the maximum measured temperature of the motor are shown in Tables 5 and 6, respectively.

The same measurements were carried out in the case of full load conditions as well. Tables 7 and 8 show the minor effect of temperature and humidity on the wrong temperature maximum measured.

Figure-7 shows the maximum temperature measured for both scenarios (no load and full load). As expected for full load conditions, the measured temperatures are higher.

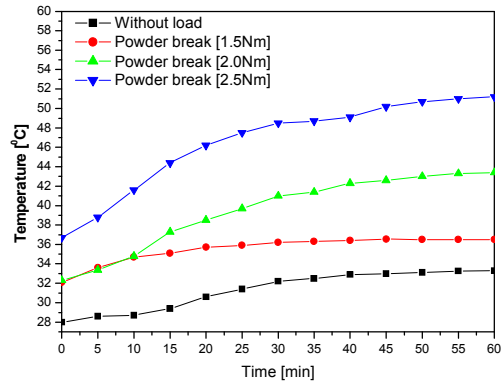


Figure.7. The Maximum Measured Temperature.

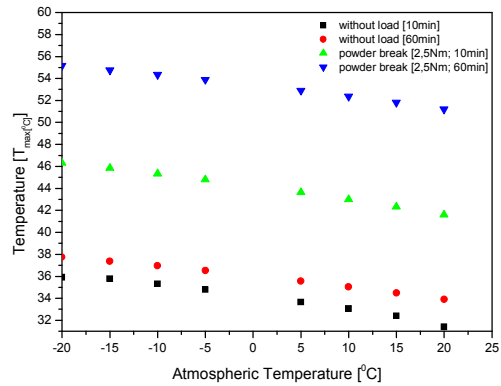


Figure.8. The Atmospheric Temperature Influence On Thermographic Measurements

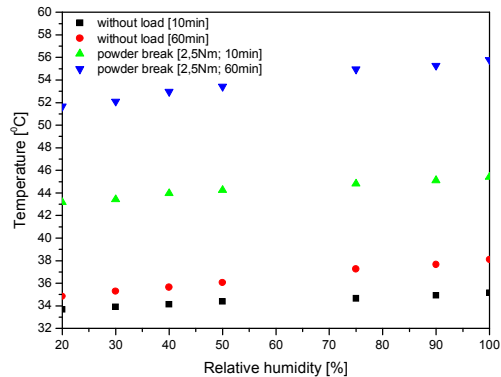


Figure.9. The Relative Humidity Influence On Thermographic Measurements

7. CONCLUSION

Wide applications in numerous sectors such as electronics, industry and engineering are attained by Thermographic Cameras. Although these cameras are able to measure temperatures very precisely if certain conditions are fulfilled, they are frequently used for rough measurements. This includes, measuring the temperature distribution on an asynchronous motor, when all that has to be found out in the first phase is which places are more thermally loaded and which are less. It is compulsory to know the surface emissivity and the distance from the measured object when the measurements are precise. The development will probably proceed in the direction of increasing the resolution of acquired images. The motor tested under different conditions and the influence of environmental parameters on the accuracy of the measurements was also investigated.

NOMENCLATURE

W_{BB} : Black-body spectral radiant Emittance

$[W/m^2]$

W_{GB} : Gray Body Spectral Radiant Emittance

$[W/m^2]$

λ : Wavelength [μm]

T_{refl} : Reflected Ambient Temperature [$^{\circ}C$]

T_{atm} : Atmosphere Temperature [$^{\circ}C$]

T_{obj} : Temperature Objects [$^{\circ}C$]

T_{max} : Maximum Temperature [$^{\circ}C$]

T_{min} : Minimum Temperature [$^{\circ}C$]

T_{av} : Average Temperature [$^{\circ}C$]

ε : Emissivity

σ : Constant Stefan-Boltzmann

$5,6697.10^{-8} W/m^2k^2$

ACKNOWLEDGMENT

This material is based on work partially supported by the technological platform PFT2M, the Industrial Engineering Laboratory and the Mechanical Production of the National School of Applied Science ENSA-Department of Industrial and finally the LDOM in Oujda.

REFERENCES

- [1] A. Benbouaza, B. Elkihel & F. Delaunois. « Analysis and diagnosis of the different defects of asynchronous machines by vibration analysis », *International Journal on Computer Science and Engineering*, Vol. 5, No.4, pp. 258-269, 2013
- [2] H. Elmaati, A. Benbouaza, B. El Kihel & F. Delaunois. « Development of a Vibration Monitoring System for Optimization of the Electrical Energy Production », *International Journal on Computer Science and Engineering*, Vol. 5, No. 6, pp. 578-589, 2013
- [3] H.Elmaati, A.Benbouaza, B.Elkihel & F. Delaunois. « Implementation of a Vibration monitoring system of a steam turbine for optimization of the maintenance », *International Journal of Emerging Trends & Technology in Computer Science*, Vol. 2, No. 6, pp. 240-245, 2013
- [4] F. Jeffali, B. El Kihel, A. Nougouai & F. Delaunois. « Monitoring and diagnostic misalignment of asynchronous machines by Infrared Thermography », *J. Mater. Environ. Sci.* Vol. 6, No 4, pp. 1192-1199, 2015
- [5] F. Jeffali, B. El Kihel, A. Nougouai & F. Delaunois, « Diagnosis of the three-phase asynchronous machine by infrared thermography technology », *Congrès International de Génie Industriel et Management des Systèmes (CIGIMS)*, EST-Fes, Morocco (2015) May 21, 22 and 23.
- [6] Ho-Jong Kim, Dong-Pyo Hong And Won-Tae Kim, « A Study on Real-Time Fault Monitoring Detection Method of Bearing Using the Infrared Thermography », *Journal of The Korean Society for Nondestructive Testing*, Vol .33, No. 4, pp.330-335, 2013
- [7] Jin-Ju Seo, Dong-Pyo Hong and Won-Tae Kim, « Study on NDT Fault Diagnosis of the Ball Bearing under Stage of Abrasion by Infrared Thermography », *Journal of The Korean Society for Nondestructive Testing*, Vol. 32, No. 1, 2012, pp.7-11, 2012
- [8] Armando Guadalupe Garcia-Ramirez, Luis Alberto Morales-Hernandez, Roque Alfredo Osornio-Rios, Juan Primo Benitez-Rangel, Arturo Garcia-Perez, Rene de Jesus Romero-Troncoso, « Fault detection in induction motors and the impact on the kinematic chain through thermographic analysis », *Electric Power Systems Research*, 114 (2014), pp. 1–9, 2014



- [9] S. Bagavathiappan, B.B. Lahiri, T. Saravanan, John Philip, T. Jayakumar, « Infrared thermography for condition monitoring – A review », *Infrared Physics & Technology*, vol. 60, pp. 35–55, 2013
- [10] C.A. Balaras, A.A. Argiriou, « Infrared thermography for building diagnostics », *Energy and Buildings*, Vol. 34, No.2, pp. 171–183, 2002
- [11] Mohd Shawal Jadin, Soib Taib, Kamarul Hawari Ghazali, « Feature extraction and classification for detecting the thermal faults in electrical installations », *Measurement*, Vol. 57, pp. 15-24, 2014
- [12] A. Nougouai, « Light, Matter, Radiation and their Interactions », *2015 Legal deposit Mo 2382*, ISBN 978-9954-35-840-5, 2015
- [13] Dennis D. Soerensen , Sønnik Clausen , James B. Mercer, Lene J. Pedersen , « Determining the emissivity of pig skin for accurate infrared thermography », *Computers and Electronics in Agriculture*, Vol.109, pp. 52–58, November 2014
- [14] A. S. Nazmul Huda, Soib Bin Taib, and Dahaman Bin Ishak, « Necessity of Quantitative Based Thermographic Inspection of Electrical Equipments », *PIERS Proceedings*, pp. 1852 - 1855, March 27-30, Kuala Lumpur, MALAYSIA 2012
- [15] Marcin BARANSKI, Artur POLAK, « Thermal diagnostic in electrical machines », *Electrical Review*, ISSN 0033-2097, Vol. 10, No. 87, 2011
- [16] A. S. Nazmul Huda, Soib Bin Taib, and Dahaman Bin Ishak, « Analysis and Prediction of Temperature of Electrical Equipment for Infrared Diagnosis Considering Emissivity and Object to Camera Distance Setting Effect », *PIERS Proceedings*, pp. 1856 - 1859, March 27-30, Kuala Lumpur, MALAYSIA 2012